Synthesis of 2,2′:5′,2″-terpyridine and 2,2′:5′,2″:5″,2‴-quaterpyridine and their photocatalysis of the reduction of water

Shozo Yanagida,*[a] Tomoyuki Ogata,[a] Yasuhiro Kuwana,[a] Yuji Wada,[a] Kei Murakoshi,[a] Akito Ishida,[b] Setsuo Takamuku,[b] Mitsuhiro Kusaba[c] and Nobuaki Nakashima[c]

[a] *Material and Life Science, Graduate School of Engineering, Osaka University, Suita, Osaka 565, Japan*
[b] *Institute of Scientific and Industrial Research, Osaka University, Ibaraki, Osaka 567, Japan*
[c] *Institute of Laser Engineering, Osaka University, Suita, Osaka 565, Japan*

2,2′:5′,2″-Terpyridine (OPy-3) and 2,2′:5′,2″:5″,2‴-quaterpyridine (OPy-4) are prepared by Ni^0-complex-catalysed polycondensation of 2,5-dichloropyridine in the presence of an excess of 2-chloropyridine. These two compounds show more efficient photocatalysis of H_2 evolution by the reduction of water than *p*-terphenyl and *p*-quaterphenyl in the presence of triethylamine as an electron donor, and $RuCl_3$ or K_2PtCl_6 as a source of Ru^0 or Pt^0 colloids which function as an electron mediator. The primary photochemical processes of OPy-*n* (*n* = 3 or 4) and the successive reactions have been investigated by γ-radiolysis, pulse radiolysis and laser flash photolysis. The OPy-*n* molecules are converted to their anion radicals through reductive quenching of the excited states. A mechanism for the photocatalysis of hydrogen evolution is proposed in which the anion radicals supply electrons to protons on the metal colloids. The anion radicals undergo protonation in competition with electron transfer, resulting in the loss of photocatalytic activity.

In recent years, a number of organic polymers with conjugated π-electrons have been synthesized and some novel properties have been successfully developed.[1–4] It was previously reported that insoluble poly(*p*-phenylene) (PPP) shows heterogeneous photocatalysis for *cis–trans* photoisomerization of simple olefins,[5] and for the photoreduction of water, ketones and olefins in the presence of triethylamine (TEA) as a sacrificial electron donor.[6] Mechanistic investigation using soluble oligo(*p*-phenylene)s (OPP-*n*,*n* denotes the number of the phenyl rings in a molecule), such as *p*-terphenyl (OPP-3) and *p*-quaterphenyl (OPP-4), revealed that their anion radicals, produced by reductive quenching, play an important role as a strong reducing intermediate in their photocatalysis under UV light irradiation.[7]

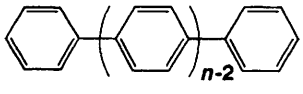

Poly(*p*-phenylene):(PPP)

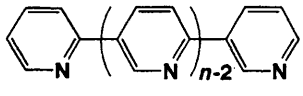

Poly(pyridine-2,5-diyl):(PPy)

Yamamoto *et al.* reported that the dehalogenation polycondensation of 2,5-dibromopyridine with zero valent Ni complexes gave poly(pyridine-2,5-diyl) (PPy).[8–10] PPy shows a single π–π* absorption band at λ_{max} = 420 nm in the solid state and possesses a linear rod-like structure. We previously reported that such PPy compounds show superior photocatalysis to those of PPP; water and some carbonyl compounds are photoreduced to H_2 and the corresponding alcohols under visible light irradiation with higher quantum efficiency.[11,12] Participation of hydride transfer was proposed as the mechanism of the photocatalysis on the basis of the following three experimental results; (i) the presence of a long-lived hydride species was inferred on the basis of the change in the UV–VIS absorption spectrum under photocatalytic conditions, (ii) benzophenone can be reduced in the pre-irradiated PPy–TEA system *in the dark* and (iii) pinacol derivatives are scarcely formed in the PPy-catalysed photoreduction of carbonyl compounds.

These findings and observations prompted us to prepare oligomeric pyridine-2,5-diyl chain compounds and to investigate their photocatalysis. This paper reports the superior photocatalysis of the oligomeric derivatives of PPy to OPP-*n* and deals with their photophysical properties and primary photochemical processes by comparing them with those of *p*-terphenyl (OPP-3) and *p*-quaterphenyl (OPP-4).

Results

Synthesis of OPy-*n*

Yamamoto *et al.* reported the synthesis of PPy by dehalogenation polycondensation of 2,5-dibromopyridine using zero valent nickel complexes as dehalogenation reagents.[8] Stirring a mixture of 2,5-dibromopyridine and $Ni(PPh_3)_4$ in a solution at 333 K gave precipitates of PPy. We first attempted the synthesis of oligomeric pyridine compounds using the same starting reagents and by varying the reaction conditions such as temperatures, reaction times, solvents, and concentrations of the Ni^0 complex. However, bipyridine or PPy was produced and no oligomeric compounds were obtained under any conditions we examined.

Synthesis of the oligopyridines was successfully performed by polycondensation of dihalogenated pyridine only in the presence of an excess amount of 2-chloropyridine. Stirring a DMF solution of 2,5-dichloropyridine, 2-chloropyridine and the Ni^0 complex gave a mixture containing the oligopyridines (Scheme 1). 2,2′:5′,2″-Terpyridine (OPy-3) and 2,2′:5′,2″:5″,2‴-quaterpyridine (OPy-4) were isolated after purification by column chromatography. These oligomers

Table 1 Physical and spectral characteristics of OPy-*n* and OPP-*n* in solution[a]

Compound	λ_{max}(log ε)[b]/nm	E_m[c]/nm	E_g[d]/eV	Φ_{EM}[e]	Solubility/g l^{-1}
OPy-3	309 (4.47) 297 (4.75)[g]	358	3.8	0.017[f]	189
OPy-4	326 (4.61) 307 (5.01)[g]	374	3.5	0.17[h]	16.2
OPP-3	286 (3.48)	341	4.0	1.0[i]	37.5
OPP-4	302 (4.51)	369	3.7	0.8[i]	0.73

[a] Measured in THF. [b] λ_{max} is the absorption maximum wavelength and ε is the extinction coefficient. [c] Emission maximum wavelength. [d] Energy gap estimated from the 0–0 transition in the spectral data measured in THF. [e] Quantum efficiency of the fluorescence. [f] Measured in ethanol. [g] Estimated by ZINDO. [h] Measured in cyclohexane. [i] See ref. 14.

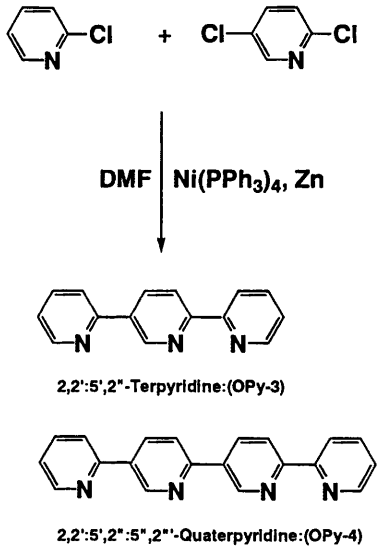

Scheme 1

possess a pyridine ring connected inversely at one end of the chain.

Spectral and physical characteristics of OPy-*n*

OPy-3 and OPy-4 were more soluble in organic solvents [tetrahydrofuran (THF), methanol (MeOH), *N*,*N*-dimethylformamide (DMF)] than OPP-*n* (Table 1). The absorption spectra of OPy-3 and OPy-4 were measured in THF and compared with those of OPP-*n*. The absorption spectra of the OPy-*n* series occurred at longer wavelengths than those of OPP-*n*.

The absorption maxima and coefficients were predicted for OPy-3 and OPy-4 by ZINDO and are listed in Table 1; the predicted values were similar to the experimental ones. The shift to a longer wavelength in the absorption maximum of OPy-4 compared with OPy-3 was reproduced in the predicted absorption spectrum. These absorption peaks of OPy-3 and OPy-4 are attributed to the π–π^* transition on the basis of the ZINDO analysis and this assignment is supported by the experimental observation that the absorption of these compounds is not affected by the change of the polarity of solvent between DMF, THF and cyclohexane.

The maxima of the fluorescence spectra of OPy-*n* also shifted to a longer wavelength than the corresponding OPP-*n* (Table 1). The quantum efficiencies of the fluorescence were much lower than OPP-*n*. The low quantum efficiencies indicate the presence of more efficient paths for relaxation of the excited singlet state of OPy-*n*. OPy-3 and OPy-4 phosphoresced with two maxima at 482 and 515, and 510 and 547 nm, respectively. The lifetimes of the phosphorescence were determined at 77 K in THF to be 1.5 and 1.0 s for OPy-3 and OPy-4, respectively. Taking into account the fact that thermal deactivation of the excited singlet state of aromatic compounds is generally negligible, the excited singlet state of the OPy-*n* compounds is considered to undergo efficient intersystem crossing to their triplet state.

Table 2 Electronic structures of OPy-*n* and OPP-*n*

Compound	E_g[a]	E_{red}[b]	E_{ox}[b,c]
OPy-3	3.8	−2.00[d]	1.8
OPy-4	3.5	−1.85[d]	1.7
OPP-3	4.0	−2.45[e]	1.6
OPP-4	3.7	−2.33[e]	1.4

[a] See Table 1. [b] V *vs.* SCE. [c] Oxidation potentials were calculated as $E_{ox} = E_{red} + E_g$. [d] Measured in acetonitrile. [e] See ref. 13.

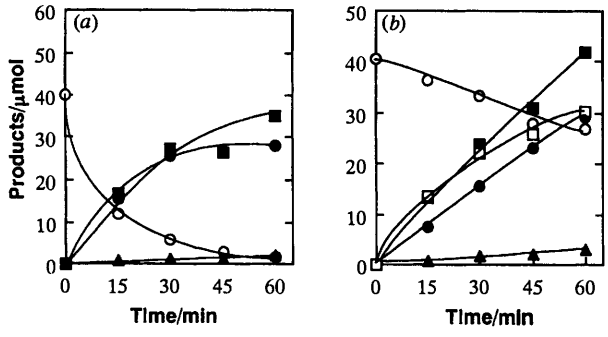

Fig. 1 Time–conversion plots for H_2 photoevolution catalysed by OPy-3 (*a*) and OPy-4 (*b*); consumption of OPy-n (○), formation of H_2 (●); ethanol (▲), diethylamine (■) and acetaldehyde (□). The DMF solution containing OPy-*n* (5 μmol), TEA (0.5 ml), H_2O (0.5 ml) and $RuCl_3$ (2.5 μmol) was irradiated at $\lambda > 290$ nm. The amount of acetaldehyde was determined only for OPy-4.

To evaluate the energy structures of OPy-*n*, their reduction potentials were measured by a voltammetric technique. The OPy-3–OPy-3$^{\bullet -}$ couple was observed as a reversible peak at $E_{\frac{1}{2}} = -2.00$ V (*vs.* SCE). In the case of OPy-4, two reversible peaks were observed at $E_{\frac{1}{2}} = -1.85$ V and −2.15 V, respectively. The first peak is attributed to the OPy-4–OPy-4$^{\bullet -}$ couple and the second peak at $E_{\frac{1}{2}} = -2.15$ V might be the OPy-4$^{\bullet -}$–OPy-4^{2-} couple.

On the measurement of the oxidation potentials, irreversible peaks were observed around 2.0 V *vs.* SCE for both OPy-3 and OPy-4. Because irreversible waves make the accuracy of E_{ox} doubtful, the energy structures of OPy-*n* were evaluated by using the energy gap estimated from the 0–0 transition measured in a DMF solution (E_g in Table 1), and are summarized along with those of OPP-*n*[13] in Table 2.

Photoreduction of H_2O

Taking into account the role of a colloidal noble metal as an electron mediator in the OPP-*n* catalysed photoreduction of H_2O,[14] OPy-*n* catalysed photoevolution of H_2 was examined in the presence of $RuCl_3$ as a source of colloidal Ru^0. Fig. 1(*a*) and 1(*b*) show the time–conversion plots for OPy-3 and OPy-4

Table 3 Quantum yields for H_2 photoevolution catalysed by oligopyridines[a] and oligophenylenes[a,b]

Catalyst	Solvent	Φ	Catalyst	Solvent	Φ
OPy-3[c]	THF	4.7×10^{-3}	OPP-3[c]	THF	1.6×10^{-4}
OPy-3[c]	DMF	9.2×10^{-2}	OPP-3[c]	DMF	6.4×10^{-4}
OPy-4[d]	THF	1.0×10^{-2}	OPP-4[d]	THF	5.8×10^{-4}
OPy-4[d]	DMF	2.1×10^{-2}	OPP-4[d]	DMF	4.4×10^{-3}

[a] Irradiated at $\lambda = 313$ nm in the presence of $RuCl_3$ (8.3×10^{-4} mol dm^{-3}). [b] Reported in ref. 14. [c] [OPy-3] = [OPP-3] = 1.67×10^{-3} mol dm^{-3}. [d] [OPy-4] = [OPP-4] = 3.3×10^{-4} mol dm^{-3}.

catalysed photoreduction of water to H_2 in aqueous DMF. Turnover numbers (TN) of OPy-3 and OPy-4 for the evolution of H_2 on the basis of the initial amounts of the photocatalysts (5 μmol) reached 6 within 1 h of irradiation. During H_2 photoevolution, comparable amounts of diethylamine (DEA) and acetaldehyde were formed, due to hydrolysis of the initial oxidation product of TEA, $[Et_2NCHCH_3]^+$.[6] A small amount of ethanol was formed through reduction of acetaldehyde.[14]

The photocatalytic activities observed in aqueous THF were lower, and the oligomers were more rapidly consumed, than in DMF. OPy-3 showed a comparable activity with OPy-4 at the early stages of the reaction, but underwent more rapid photodegradation under UV irradiation, resulting in a lowering of the total activity for H_2 evolution.

Photolysis in D_2O-containing DMF with OPy-3 or OPy-4 gave a mixture of D_2, DH and H_2 in 79:13:8 or 74:12:14 ratios, respectively, indicating that the major source of the hydrogen is water. For both OPy-3 and OPy-4, H_2 evolution was almost negligible in the absence of $RuCl_3$. When $RuCl_3$ was replaced with Ru colloids prepared in advance according to the reported method,[14] H_2 formation was observed as well. When K_2PtCl_6 was employed as a precursor of the electron mediator instead of $RuCl_3$, a comparable amount of hydrogen was evolved.

The quantum yields at $\lambda = 313$ nm for the formation of H_2 were measured to compare the intrinsic photocatalytic activity of OPy-*n* with that of OPP-*n* under comparable conditions. As shown in Table 3 both OPy-3 and OPy-4 systems showed larger quantum yields than that of OPP-3 or OPP-4.

The following experiments ruled out the possibility that ruthenium complexes such as $Ru(OPy\text{-}n)_3^{2+}$ might form from OPy-*n* and Ru salt in the system, with the resulting complex photosensitizing the H_2 evolution; when the reaction systems containing OPy-3, OPy-4 or $Ru(bpy)_3^{2+}$ were irradiated by UV light, H_2 evolution was observed for all the systems. However, H_2 evolution photocatalysed by OPy-3 or OPy-4 ceased completely when the UV region of the irradiating light was removed by a UV-cut filter (Fig. 2).[15]

Photochemistry of OPy-3 and OPy-4

Fluorescence from OPy-3 and OPy-4 was quenched by TEA. A Stern–Volmer plot gave a linear correlation. The slopes of the plots, k_{sv}, were 1.4 dm^3 mol^{-1} (in MeOH) for OPy-3, and 9.3 dm^3 mol^{-1} (in THF), 9.6 dm^3 mol^{-1} (in DMF) and 3.0 dm^3 mol^{-1} (in MeOH) for OPy-4. Because the lifetime of fluorescence of OPy-4 was determined to be below 1 ns, the rate constants for the quenching process of the excited singlet state of OPy-4 by TEA were estimated to be in the order of 10^9–10^{10} dm^3 mol^{-1} s^{-1}.

The absorption spectra of the anion radicals of OPy-3 (OPy-$3^{\bullet -}$) and OPy-4 (OPy-$4^{\bullet -}$) were measured by the γ-radiolysis technique at 77 K (Fig. 3). Both the OPy-$3^{\bullet -}$ and OPy-$4^{\bullet -}$ gave clear absorption bands. The absorption maximum of OPy-$4^{\bullet -}$ shifted to a longer wavelength than that of OPy-$3^{\bullet -}$ in a similar manner as reported for the anion radicals of OPP-*n* (*n* = 3, 4).[7]

Semi-empirical MO calculations with MOPAC generated a planar conformation of the three rings in OPy-$3^{\bullet -}$ as the energetically optimized structure. Fig. 4 displays the absorption spectrum of OPy-$3^{\bullet -}$ predicted by ZINDO for the conformation obtained as the most stable structure by MOPAC. The shape of the spectrum with its two maxima at around 480 nm and above 800 nm is very similar to that of the observed one in Fig. 3(*a*).

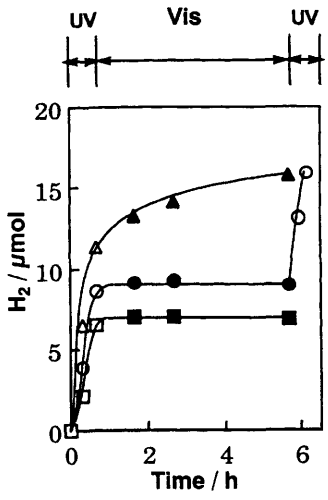

Fig. 2 Photoevolution of H_2 under irradiation by UV or VIS light. The sample solutions were irradiated at $\lambda > 290$ nm and then irradiated at $\lambda > 400$ nm as displayed in the figure. Yields of H_2 are shown as open symbols under UV-light irradiation and as closed symbols under visible-light irradiation. Each sample contained either OPy-3 (□, ■), OPy-4 (○, ●), or $Ru(bpy)_3^{2+}$ (△, ▲) as a photosensitizer.

When the cold matrices including the anion radicals were warmed up gradually, the absorption due to the anion radicals decreased and a peak at 412 nm and a broad one at 620 nm grew up for OPy-3. As for OPy-4, a weak shoulder peak was observed at 430 nm during warming of the matrix, but a broad one at the longer wavelength was indistinguishable [Fig. 3(*b*)]. These new absorption peaks which appeared during warming could be assigned to protonated radicals formed by protonation of the anion radicals.

In order to confirm the assignment, the absorption spectra of the protonated radicals of OPy-3 were predicted with ZINDO calculations. The spectra for the radicals formed by protonation at the 1′ (N atom) and 4′ positions of the anion radical are displayed in Fig. 4. The protonated radical showed a strong absorption at around 350 nm and a broad, weak one at around 680 nm according to the ZINDO calculations. The shift of the absorption peaks of the protonated radicals to a shorter wavelength compared with the anion radicals is probably due to loss in conjugation in the protonated radical. The shape obtained from the ZINDO calculations consisting of a strong peak and a broad but weak peak is very similar to that obtained during warming of the cold matrix.† These results lead to the conclusion that the anion radical of OPy-3 formed in THF or DMF is readily converted to the protonated radicals (Scheme 2).

The reactivity of OPy-$n^{\bullet -}$ was investigated by the pulse radiolysis technique. Figs. 5 and 6 show the transient absorption spectra of OPy-$3^{\bullet -}$ and OPy-$4^{\bullet -}$ in THF and in DMF at appropriate delay times after the pulse, respectively. In all the four systems (OPy-3–THF, OPy-3–DMF, OPy-4–THF and OPy-4–DMF), the absorption spectra observed in the early

† Some deviation in the positions of the peaks between the observed and the predicted spectra could be due to the poor reproducibility of the absolute values in the electronic structures, still unsolved not only in ZINDO but also in other MO programs and the different environments around the radical (ZINDO calculations are based on a molecule in a vacuum).

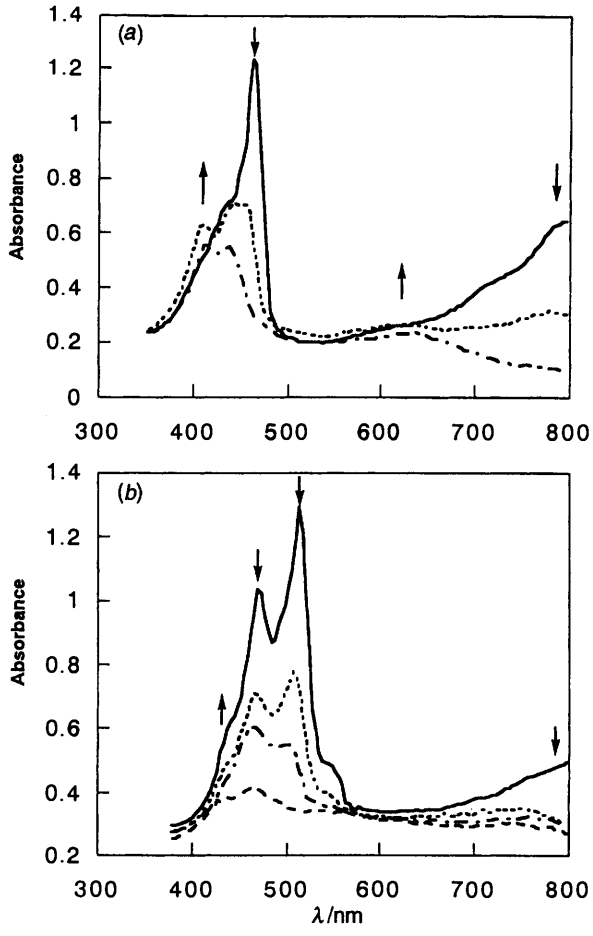

Fig. 3 Absorption spectra of the anion radicals of OPy-3 (*a*) and OPy-4 (*b*) formed by γ-ray irradiation in methyltetrahydrofuran frozen at 77 K. After the spectra were recorded at 77 K (solid line), changes of the spectra were recorded with increasing temperature in the order of the short-dashed line, the dashed and dotted line, and the long-dashed line. The arrows indicate changes in the absorption peaks on warming.

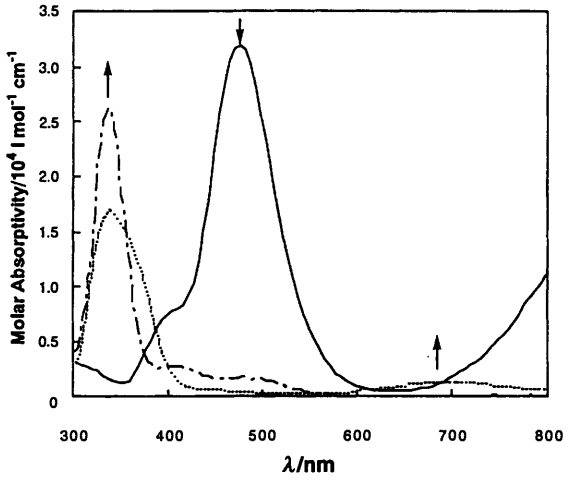

Fig. 4 Absorption spectra predicted by ZINDO for the anion radical (OPy-3'$^-$) and the radicals protonated at the 1' and 4' positions; the anion radical (solid line), the radical protonated at 1' (dotted line) and at 4' (dashed and dotted line). The arrows indicate changes in the absorption peaks from the cation radical to the protonated radical.

stages were almost identical with those of the anion radicals shown in Fig. 3. Each spectrum consisted of two peaks; a peak at 460 nm with a shoulder at lower wavelength and a broad peak above 600 nm for OPy-3, and a peak at 510 nm with a shoulder at lower wavelength and a broad peak above 800 nm for OPy-4. In the transient spectra of OPy-3, a peak at 410 nm and a broad one at 620 nm clearly grew up at 300 ns after the

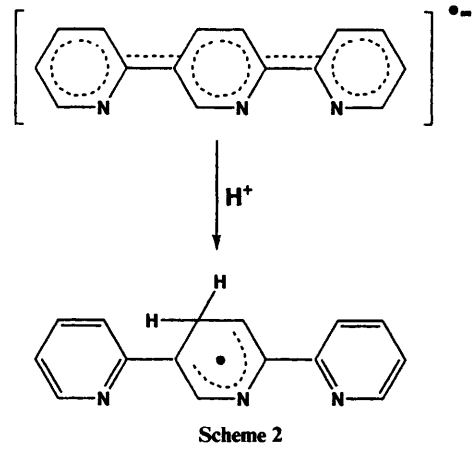

Scheme 2

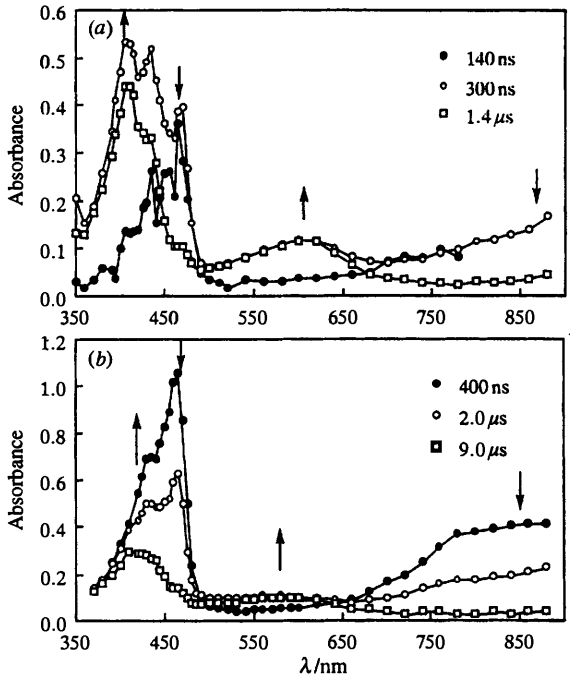

Fig. 5 Transient absorption spectra of OPy-3 in THF (*a*) and DMF (*b*) solutions (10 mmol) observed by pulse radiolysis. The spectra were recorded at various delay times after the pulse as displayed in the figure. The arrows indicate changes in the absorption peaks with the delay time.

pulse in THF. Similar changes in the spectra were observed in DMF. As for OPy-4, the rise of a new peak at 450 nm and a broad one at 710 nm was observed with a decrease of the absorption due to the anion radical of OPy-4. The wavelengths of the new peaks coincided with those of the peaks observed in the γ-radiolysis. These observations indicate that the anion radicals of OPy-*n* are converted to their protonated radicals through protonation not only in the cold matrices but also in the solutions at room temperature within several μs.

The decay of the transient absorption of OPy-*n*$^{\bullet -}$ in the presence of $RuCl_3$ or H_2PtCl_6 was observed for the pulse radiolysis in DMF. The addition of the metal salts accelerated the decay, which followed pseudo-first-order kinetics. A linear relation of the pseudo-first-order rate constant *vs.* the concentrations of the metal salts gave the second-order rate constants: 4×10^9 dm^3 mol^{-1} s^{-1} for OPy-3$^{\bullet -}$ and 3×10^9 dm^3 mol^{-1} s^{-1} for OPy-4$^{\bullet -}$ in the presence of $RuCl_3$ (up to 2.0×10^{-3} mol dm^{-3}); 2×10^9 dm^3 mol^{-1} s^{-1} for OPy-4$^{\bullet -}$ in the presence of H_2PtCl_6 (up to 4.0×10^{-3} mol dm^{-3}).

A laser pulse photolysis technique was employed to ensure the formation of the anion radicals of OPy-*n* in the photocatalytic system and to examine their behaviour. When OPy-4 was irradiated by a pulse of 308 nm in DMF, an absorption

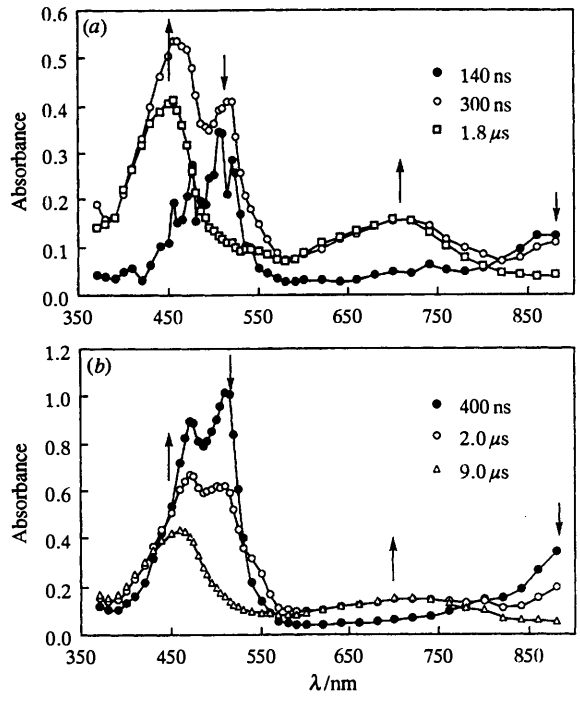

Fig. 6 Transient absorption spectra of OPy-4 in THF (*a*) and DMF (*b*) solutions (5 mmol) observed by pulse radiolysis. The spectra were recorded at various delay times after the pulse as displayed in the figure. The arrows indicate changes in the absorption peaks with the delay time.

with a maximum at 520 nm was observed. This absorption peak is attributed to the T–T transition of OPy-4, since OPy-4 shows a weak fluorescence and a strong phosphorescence.

The formation of the anion radical showing an absorption maximum at 510 nm was observed for OPy-4 in the THF or DMF solution containing TEA (Fig. 7). Another absorption with a peak at 450 nm was also observed especially for the THF solution, demonstrating the same change of the anion radical to the protonated radical in the photocatalytic system as observed in the radiolysis experiments. When K_2PtCl_6 was added to the system, the decay of the absorption of the anion radical was accelerated. The pseudo-first-order rate constant was determined to be 3×10^9 dm^3 mol^{-1} s^{-1} from the dependence of the decay on the concentration of K_2PtCl_6 (up to 4×10^{-4} mol dm^{-3}). This value coincided with that obtained in the pulse radiolysis experiments. A similar experiment using $RuCl_3$ failed, because the absorption of $RuCl_3$ interfered with the measurement of the absorption of the anion radical.

Discussion

As long as dihalogenated pyridine was used as a starting compound for the polycondensation of pyridine rings, only PPy or bipyridine was produced under any of the conditions we employed. A mechanism for the polycondensation in the system has been reported in which oxidative addition of the halogenated aryl compounds to the Ni catalyst, in the form of $Ni^0(PPh_3)_3$, occurs and then the aryl groups are coupled in the coordination sphere.[16,17] Oxidative addition of a second halogenated aryl compound to the Ni complex already coordinated by the first one is rate-determining and successive coupling of the aryl group is fast in the polycondensation of halogenated aryl compounds. This could explain the failure of the synthesis of oligomers using only dihalogenated pyridine.

The absorption peaks of OPy-*n* occur at a longer wavelength than those of the corresponding OPP-*n*. OPy-*n* will favour a planar structure in the ground and the excited state due to less steric hindrance between hydrogens of the neighbouring pyridine rings than OPP-*n*. The shift of the absorption peak to a longer wavelength with an increase in the chain length from OPy-3 to OPy-4 suggests a wider extent of conjugation in OPy-4 than in OPy-3. These facts support the conclusion that the twisting angle between the rings determined by the steric hindrance of the closest hydrogen atoms remarkably affects the π–π^* electronic excitation energy of OPy-*n*.

Table 4 Heats of formation of the OPy-*n* and OPP, and their anion radicals calculated by MOPAC[a]

	H(N)[b]	H(AR)[c]	ΔH[d]
OPy-3	94.51	59.86	−34.65
OPy-4	126.40	87.01	−39.39
OPP-3	72.68	46.67	−26.01
OPP-4	97.28	67.11	−30.17

[a] The structures were obtained by energetic optimization. [b] Heats of formation (kcal mol^{-1}) of the neutral molecules. [c] Heats of formation (kcal mol^{-1}) of the anion radicals. [d] $\Delta H = H(AR) - H(N)$.

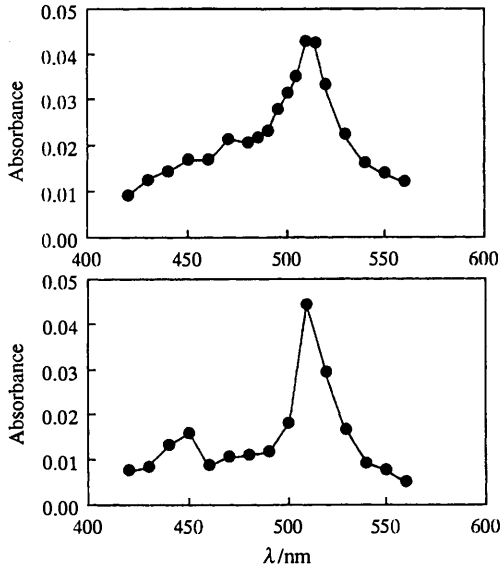

Fig. 7 Transient absorption spectra of OPy-4 in the presence of TEA obtained by laser flash photolysis: a DMF solution (*a*) and THF solution (*b*); OPy-4 (1×10^{-5} mol dm^{-3}) and TEA (1.0 mol dm^{-3})

A peculiarity observed in the photoprocess of OPy-*n* in contrast to OPP-*n* is the participation of the triplet state formed readily by the intersystem crossing of the excited singlet state. Therefore, both the excited singlet state and the triplet state should be taken into account in the photocatalysis of OPy-*n*.

The energetically optimized structure obtained by MOPAC for OPy-$n^{\bullet -}$ was completely planar as well as for OPP-$n^{\bullet -}$, which explains the shift of the absorption peak of the anion radicals of OPy-*n* to a longer wavelength with increasing chain length. The difference between the heat of formation of the anion radical and that of the neutral molecule could be regarded as a scale of the reduction potential (Table 4). The order of the reduction potential predicted from the difference is OPP-3 < OPP-4 < OPy-3 < OPy-4, which coincides with that obtained electrochemically. This order indicates that the reducing power of OPy-$n^{\bullet -}$ is lower than OPP-$n^{\bullet -}$, but it is strong enough to reduce protons into H_2.

The anion radical has been recognized to be the transient species formed from the excited states of OPy-*n* in the presence of TEA. It is considered to be formed through reductive quenching of the excited singlet state and the triplet state. This anion radical gives an electron to the noble metal ion at the initial stage of the photocatalysis.

On the basis of the observations of the photochemical reactions of OPy-*n*, a mechanism for the photoevolution of H_2 in the OPy-*n*–TEA system is deduced as shown in Scheme 3. The UV irradiation produces the excited singlet state of OPy-*n*,

$$\text{OPy-}n + h\nu \longrightarrow {}^1\text{OPy-}n^* \quad (1)$$

$${}^1\text{OPy-}n^* \longrightarrow {}^3\text{OPy-}n^* \quad (2)$$

$${}^1\text{OPy-}n^* + \text{TEA} \longrightarrow \text{OPy-}n^{\cdot -} \quad (3)$$

$${}^3\text{OPy-}n^* + \text{TEA} \longrightarrow \text{OPy-}n^{\cdot -} \quad (4)$$

$$\text{OPy-}n^{\cdot -} \longrightarrow \text{OPy-}n + \text{e} \quad (5)$$

$$3\text{e} + \text{RuCl}_3 \longrightarrow \text{Ru}^\circ \quad (6)$$

$$\text{e} + \text{H}^+ \xrightarrow{\text{Ru}^\circ} \tfrac{1}{2}\text{H}_2 \quad (7)$$

$$\text{OPy-}n^{\cdot -} + \text{H}^+ \longrightarrow \text{OPy-}n\text{-H}^{\cdot} \quad (8)$$

Scheme 3

^{1}OPy-*n**. ^{1}OPy-*n** readily undergoes intersystem crossing and is converted to the triplet state, ^{3}OPy-*n**. ^{1}OPy-*n** and ^{3}OPy-*n** are reductively quenched by TEA to produce the anion radical, OPy-$n^{\cdot -}$, and cation radical of TEA (TEA$^{\cdot +}$). As reported previously, TEA$^{\cdot +}$ decomposes immediately to $Et_2NC{\cdot}HCH_3$ by deprotonation. This radical is oxidized to produce the cation $Et_2NC^+HCH_3$, and subsequently gives diethylamine (DEA) and acetaldehyde by hydrolysis of the cation. The electron transfer from OPy-$n^{\cdot -}$ to $RuCl_3$ or H_2PtCl_6 generates colloids of Ru or Pt, respectively. Electrons are transferred from the anion radicals to metal colloids, on which protons are reduced to H_2.[14] Protonation of the anion radical should proceed in competition with the electron transfer to metal colloids in the photocatalysis.

Lowering of the photocatalytic activity of OPy-*n* is due to photodegradation caused by protonation of the anion radical. When the protonated radical is further hydrogenated to the dihydrogenated species through electron transfer and protonation or mutual disproportionation, OPy-*n* should lose aromaticity, resulting in a loss of the photocatalysis. OPy-4 is more resistant to the photodegradation than OPy-3. The more rapid photodegradation of OPP-3 than OPP-4 was also observed in the OPP-*n* photocatalytic system (photo-Birch reduction).[14] The stability of OPP-4 is explained as being due to broader delocalization of the negative charge on the anion radical of OPP-4.[7] This should be true for the photocatalysis of OPy-4, because the absorption of the anion radical of OPy4 observed at a longer wavelength than that of OPy-3 indicates wider delocalization of the electron on the anion radical of OPy-4, as substantiated by the planar conformation obtained by the MO calculations.

OPy-*n* shows much higher photocatalytic activity for water reduction to H_2 than OPP-*n*. This fact is in agreement with the more efficient photocatalysis of PPy than PPP.[12] When taking into account the two results—the comparable rate constant of OPy-*n* (10^9–10^{10} dm^3 mol^{-1} s^{-1}) and OPP-*n* (3×10^9 dm^3 mol^{-1} s^{-1})[14] for the reductive quenching process of the excited singlet state by TEA, and the lower rate constants, by one fold, for the electron transfer from the anion radicals of OPy-*n* (2–4×10^9 dm^3 mol^{-1} s^{-1}) to metal salts than OPP-*n* (3×10^{10} dm^{-3} s^{-1})—the high photocatalytic activity of OPy-*n* would be attributed to participation of their triplet states in the mechanism of the photocatalysis. The triplet state would be quenched reductively by TEA and converted more efficiently to the anion radicals than the excited singlet state, because it is longer-lived than the excited singlet state.

Because OPy-*n* absorbs only UV-region light overlapping the absorption band of carbonyl compounds, an experiment cannot be carried out examining whether OPy-*n* photocatalyses reduction of carbonyl compounds as well as PPy. No evidence has been obtained for participation of hydride transfer in the photocatalytic H_2 evolution with OPy-*n*. PPy is considered to undergo protonation of its anion radical formed in the polymer chain as is observed for the oligomers. The protonated radical of OPy-*n* found in the present work could be a precursor of the dihydrogenated species functioning as a supplier of hydride in the photocatalysis of PPy. The polymeric structure of PPy may be a requisite for converting the protonated radical into the dihydrogenated species by giving another electron from the anion radical formed in the same chain.[12]

Experimental

Materials

2-Chloropyridine, 2-bromopyridine and 2,5-dibromopyridine obtained from Tokyo Kasei, 2,5-dichloropyridine and zinc powder from Aldrich Chemical Company, *p*-terphenyl (OPP-3), *p*-quaterphenyl (OPP-4), ruthenium (Ru) and ruthenium chloride ($RuCl_3$), from Nacalai Tesque, were used without further purification. The other chemicals used in this study were identical to those used in the previous studies.[6,14]

Analysis

H_2 was analysed by GC using a 2 m × 3 mm activated carbon column on a Shimadzu Model GC-12A (carrier gas, Ar; column temperature, 373 K, injection temperature, 423 K). Products in the liquid phase were analysed by GLC using a Shimadzu Model GC-7A apparatus equipped with a flame ionization detector and the following columns (carrier gas N_2); a 0.5 m × 3 mm OV-17 column for OPy-*n* (for OPy-3: carrier flow, 30 ml min^{-1}; column temperature, 503 K; injection temperature, 523 K. For OPy-4: carrier flow, 40 ml min^{-1}; column temperature, 543 K; injection temperature, 573 K); a 3 m × 3 mm ASC-L column for diethylamine and ethanol (carrier flow, 20 ml min^{-1}, column temperature, 453 K; injection temperature, 473 K).

GC mass analysis was conducted on JEOL JMS-DX. ^{1}H NMR data were obtained on a JEOL JNM-GSX 400 spectrometer. *J* Values are given in Hz. UV–VIS spectra were recorded on a Hitachi Model 220A spectrophotometer. Steady-state photoluminescence spectra were obtained on a Hitachi Model 850 spectrophotometer. Fluorescence quantum yields were determined by using naphthalene and anthracene as standard reagents.

Cyclic voltammetry was carried out on a potentiostat (Nikko Keisoku NPOT-2501) with a potential sweeper (Nikko Keisoku NPS-2A) or on a BAS 100 instrument with a scan rate of 100 mV s^{-1}. The sample solutions contained 1 mmol dm^{-3} OPy-*n* and 0.1 mol dm^{-3} tetrapropylammonium perchlorate in acetonitrile. A two-compartment cell, a glassy carbon working electrode, a platinum wire counter electrode, and a saturated calomel reference electrode (SCE) were employed.

Synthesis of OPy-3 and OPy-4

A DMF solution (60 ml) of $NiCl_2$ (1.85 g, 14.3 mmol), PPh_3 (26.24 g, 100 mmol) and Zn powder (13.16 g, 204 mmol) was heated at 323 K for 1 h with stirring under dry argon. To the resulting red–brown suspension was added a solution of 2-chloropyridine (23.08 g, 203 mmol) and 2,5-dichloropyridine (5.95 g, 40.2 mmol) in DMF (10 ml), and the mixture was stirred at 348 K. After 12 h, the reaction mixture was stirred with aqueous NaOH (200 ml) and extracted with chloroform. The extract was evaporated to give an oily mixture of OPy-3 and OPy-4. To eliminate PPh_3, column chromatography was undertaken using a neutral-alumina column and Et_2O–MeOH (95:5) as an eluent, and then OPy-3 and OPy-4 were carefully separated by flash chromatography using a neutral-alumina column and chloroform as eluent.

OPy-3 (1.7 g, 18%), mp 157–158 °C (Found: C, 77.05; H, 4.65; N, 18.0%. $C_{15}H_{11}N_3$ requires C, 77.25; H, 4.75; N,

18.0%); δ_H(400 MHz; $CDCl_3$; Me_4Si) 7.29 (1 H, ddd, 5-H), 7.32 (1 H, ddd, 5″-H), 7.80 (1 H, dd, 4′-H), 7.84 (2 H, td, 4-H and 4″-H), 8.47 (2 H, ddd, 3-H and 3″-H), 8.52 (1 H, d, 3′-H), 8.71 (1 H, ddd, 6-H), 8.75 (1 H, ddd, 6″-H), 9.29 (1 H, d, 6′-H); $J_{3,4}$ 8.0, $J_{4,5}$ 8.0, $J_{5,6}$ 4.4, $J_{3,5}$ 2.0, $J_{4,6}$ 1.5, $J_{3,6}$ 1.0, $J_{3',4'}$ 8.0, $J_{4',6'}$ 1.5, $J_{3',6'}$ 1.0, $J_{3'',4''}$ 7.8, $J_{4'',5''}$ 7.8, $J_{5'',6''}$ 4.8, $J_{3'',5''}$ 2.0, $J_{3'',6''}$ 1.0, $J_{4'',6''}$ 1.5; δ_C(100.8 MHz; $CDCl_3$; Me_4Si) 120.6, 121.0, 121.3, 122.9, 123.9, 134.7, 135.2, 137.0, 147.7, 149.3, 150.1, 154.7, 155.8, 156.3; *m/z* 233 (M^+, 100%), 155 (30, M − C_5H_5N).

OPy-4 (0.62 g, 10%), mp 228–232 °C (Found: C, 77.5; H, 4.6; N, 17.9%. $C_{20}H_{14}N_4$ requires C, 77.4; H, 4.55; N, 18.05%); δ_H(400 MHz; $CDCl_3$; Me_4Si) 7.32 (2 H, m, 5-H and 5‴-H), 7.83 (2 H, m, 4′-H and 4″-H), 7.85 (2 H, td, 4-H and 4‴-H), 8.49 (2 H, dd, 3-H and 3‴-H), 8.54 (1 H d, 3′-H), 8.59 (1 H, d, 3″-H), 8.72 (1 H, ddd, 6-H), 8.76 (1 H, ddd, 6‴-H), 9.31 (1 H, d, 6′-H), 9.34 (1 H, d, 6″-H); $J_{3,4}$ 7.8, $J_{4,5}$ 7.8, $J_{5,6}$ 4.0, $J_{3,5}$ 2.0, $J_{4,6}$ 2.0, $J_{3,6}$ 1.0, $J_{3',4}$ 8.3, $J_{3'',4''}$ 8.3, $J_{4',6'}$ 1.0, $J_{4'',6''}$ 1.0, $J_{3',6'}$ 1.0, $J_{3'',6''}$ 1.0, $J_{3''',4'''}$ 8.3, $J_{4''',5'''}$ 5.9, $J_{5''',6'''}$ 3.4, $J_{3''',5'''}$ 2.0, $J_{3''',6'''}$ 1.0, $J_{4''',6'''}$ 1.5; δ_C(100.8 MHz; $CDCl_3$; Me_4Si) 120.4, 120.5, 120.7, 121.0, 121.2, 121.4, 122.9, 123.9, 134.8, 135.2, 136.9, 137.1, 147.8, 148.5, 149.3, 150.2, 154.4, 154.7, 154.8, 155.9; *m/z* 310 (M^+, 100%), 232 (18, M − C_5H_5N), 155 (22, M − C_5H_5N–C_5H_5N).

Photoreactions

Photocatalyst (OPy-3 or OPy-4), 0.5 ml of TEA, 0.5 ml of aqueous solution (5 mmol dm^{-3}) of $RuCl_3$ and solvent (1–2 ml of THF or DMF) were placed into a Pyrex-glass tube (8 mm in diameter). After the mixture was purged with argon, the tube was closed off with a gum stopper and then irradiated under stirring at $\lambda > 290$ nm using a 500 W high-pressure mercury arc lamp.

Determination of quantum yields of photoreactions. Quantum yields were determined by using a potassium ferrioxalate actinometer. The incident light was isolated from a Xe lamp (500 W) through a WACOM XD-501S monochromator.

Pulse radiolysis

A 2 ml DMF solution of OPy-3 (10 mmol dm^{-3}) or OPy-4 (5 mmol dm^{-3}) was placed into a quartz cell. After being purged with argon, the cell was closed off with a gum stopper, then was measured by the pulse radiolysis technique in the same manner reported previously.[14]

γ-Radiolysis

A 2 ml solution of OPy-*n* (5 mmol dm^{-3}) in 2-methyltetrahydrofuran was degassed under high vacuum and sealed in a Suprasil cell. γ-Ray irradiation was carried out at 77 K by use of a ^{60}Co source. Absorption spectra were recorded on a multichannel spectrophotometer (Otsuka Electronics MCPD-1000).

Laser flash photolysis

A solution of photocatalyst was degassed thoroughly by a freeze–pump–thaw method and sealed in a quartz-made cell under vacuum. A XeF excimer laser (LAMBDA PHYSIK EMG 201 MSC) and a Xe pulse lump (7 W, 30 ns) were employed as an excitation laser source and a monitor light source.

Semi-empirical Mo calculations

Molecular modelling and displaying were handled with CHAChe system, handled by Sony/Tektronix corporation. MO calculations were carried out with MOPAC ver.6 with the parameters of PM3.[18,19] Absorption spectra were predicted with ZINDO for molecular structures energetically optimized with MOPAC/MNDO/PM3.[20]

Acknowledgements

This work was partly supported by a Grant-in-Aid for Scientific Research (A) from the Ministry of Education, Science, Sports, and Culture of Japan (No. 06403023) and partly defrayed by the Grant-in-Aid on Priority-Area-Research on 'Photoreaction Dynamics' from the Ministry of Education, Science, Sports, and Culture of Japan (No. 07228246). T. O. thanks the Japan Society for the Promotion of Science for a Research Fellowship for Young Scientists.

References

1 H. Shirakawa, D. J. Louis, A. G. MacDiarmid, C. K. Chiang and A. J. Heeger, *J. Chem. Soc., Chem. Commun.*, 1977, 578.
2 H. Shinohara, M. Aizawa and H. Shirakawa, *J. Chem. Soc., Chem. Commun.*, 1986, 209.
3 Y. Tanaka, T. Uryu, M. Ohashi and K. Tsujimoto, *J. Chem. Soc., Chem. Commun.*, 1987, 1703.
4 T. Kawai, T. Kuwabata and K. Yoshino, *J. Chem. Soc., Faraday Trans.*, 1992, **88**, 2041.
5 S. Yanagida, M. Hanazawa, A. Kabumoto, C. Pac and K. Yoshino, *Synth. Met.*, 1986, **18**, 785.
6 T. Shibata, A. Kabumoro, T. Shiragmi, S. Ishitani, C. Pac and S. Yanagida, *J. Phys. Chem.*, 1990, **94**, 2068.
7 S. Matsuoka, T. Kohzuki, C. Pac, A. Ishida, S. Takamuku, M. Kusaba, N. Nakashima and S. Yanagida, *J. Phys. Chem.*, 1992, **96**, 4437.
8 T. Yamamoto, T. Ito and K. Kubota, *Chem. Lett.*, 1988, 153.
9 T. Yamamoto, T. Maruyama and K. Kubota, *Chem. Lett.*, 1989, 1951.
10 T. Yamamoto, T. Maruyama, T. Ikeda and M. Sisido, *J. Chem. Soc., Chem. Commun.*, 1990, 1306.
11 S. Matsuoka, T. Kohzuki, A. Makahsima, C. Pac and S. Yanagida, *J. Chem. Soc., Chem. Commun.*, 1991, 580.
12 S. Matsuoka, T. Kohzuki, Y. Kuwana, A. Nakamura and S. Yanagida, *J. Chem. Soc., Perkin Trans. 2*, 1992, 679.
13 K. Meerholz and J. Heinze, *J. Am. Chem. Soc.*, 1989, **111**, 2325.
14 S. Matsuoka, H. Fujii, T. Yamada, C. Pac, A. Ishida, S. Takamuku, M. Kusaba, N. Nakashima, S. Yanagida, K. Hashimoto and T. Sakata, *J. Phys. Chem.*, 1991, **95**, 5802.
15 G. M. Brown, B. S. Brunschwig, C. Creutz, J. F. Endicott and N. Sutin, *J. Am. Chem. Soc.*, 1979, **101**, 1298.
16 G. T. Kwiatkowski, I. Colon, M. J. El-Hibri and M. Matzner, *Makromol. Chem. Macromol. Symp.*, 1992, **54/55**, 199.
17 V. Percec, C. Pugh, E. Cramer, S. Okita and R. Weiss, *Makromol. Chem. Macromol. Symp.*, 1992, **54/55**, 113.
18 J. J. P. Stewart, Quantum Chemical Program Exchange Organization, USA, Program No. 455.
19 J. J. P. Stewart, *J. Comp. Chem.*, 1989, **10**, 209.
20 W. D. Edwards and M. C. Zerner, *Theor. Chim. Acta.*, 1987, **72**, 347.

Paper 6/01023G
Received 12*th February* 1996
Accepted 17*th April* 1996